

2011

Poly-ols Based Sol-Gel Synthesis of Zinc Oxide Thin Films

Gururaj V. Naik

Purdue University, gnaik@purdue.edu

Navakanta Bhat

Indian Institute of Science, Bangalore

Follow this and additional works at: <http://docs.lib.purdue.edu/nanopub>



Part of the [Nanoscience and Nanotechnology Commons](#)

Naik, Gururaj V. and Bhat, Navakanta, "Poly-ols Based Sol-Gel Synthesis of Zinc Oxide Thin Films" (2011). *Birck and NCN Publications*. Paper 760.

<http://docs.lib.purdue.edu/nanopub/760>

This document has been made available through Purdue e-Pubs, a service of the Purdue University Libraries. Please contact epubs@purdue.edu for additional information.



Poly-ols Based Sol–Gel Synthesis of Zinc Oxide Thin Films

Gururaj V. Naik^{a,z} and Navakanta Bhat^b

^aSchool of Electrical and Computer Engineering and Birck Nanotechnology Center, Purdue University, West Lafayette, Indiana 47907, USA

^bDepartment of Electrical Communication Engineering, Indian Institute of Science, Bangalore 560012, India

We demonstrate that the structural and optical properties of a sol–gel deposited zinc oxide thin film can be tuned by varying the composition of the sol, consisting of ethylene glycol and glycerol. A systematic study of the effect of the composition of sol on the mean grain size, thickness, and defect density of the zinc oxide film is presented. About 20% glycerol content in the sol is observed to improve the quality of the film, as evaluated by X-ray diffraction and photoluminescence studies. Thus, optimizing the composition of the sol for about 60 nm thick ZnO film using 20% glycerol resulted in the zinc oxide film that is about 80% transparent in visible spectrum, exhibiting electrical resistivity of about 18 Ω cm and field-effect mobility of 0.78 cm²/(V s). © 2010 The Electrochemical Society. [DOI: 10.1149/1.3515894] All rights reserved.

Manuscript submitted October 29, 2009; revised manuscript received October 21, 2010. Published November 30, 2010.

Semiconducting oxide thin films have received significant attention for their applications in large area devices, such as displays, solar cells, and sensors. Zinc oxide, being a transparent high performance oxide semiconductor, is shown to be a suitable material for such applications.¹ Unlike most other oxide semiconductors, a zinc oxide thin film can be deposited at relatively low temperatures, which makes it an economical choice.^{2–6} Solution-processing techniques are the most attractive low-temperature deposition techniques as they start with simple metal salts and solvents and use simple processing techniques, such as spin-coating.^{5–7} Chemical bath deposition (CBD) and sol–gel deposition are the popular solution-processing techniques for depositing thin films of zinc oxide. CBD requires an initial seeding step to initiate deposition.^{4,7} But growing a uniform seeding layer is difficult. On the contrary, sol–gel deposition does not suffer from such disadvantages.

Various sol–gel synthesis routes using solvents such as isopropyl alcohol, methanol, and ethanol have been reported for thin films of ZnO.^{8–12} However, Kamalasanan and Chandra⁸ reported that the sols prepared using these alcohols do not gel properly upon hydrolysis. But the high boiling, viscous sol based on ethylene glycol is reported to overcome this problem.⁸

Several variants of ethylene glycol based sol–gel technique are reported in literature.^{8,9,11} However, tuning the properties of the ZnO thin film by modifying the composition of the sol is not reported. Sols composed of different solvents offer trade-offs in various properties of sol, such as stability, viscosity, and boiling point and hence allow tuning of the properties of the thin film.¹³ In this paper, we present a systematic study on the effects of composition of sol, composed of a mixture of ethylene glycol and glycerol, on the properties of the sol–gel deposited ZnO films. The characteristics of the ZnO film such as morphology, mean grain size, photoluminescence (PL), and film thickness are studied for various sol compositions. The paper concludes with the demonstration that the ZnO films obtained by this technique are suitable for transparent electronics.

Experimental

The solution of zinc acetate dihydrate [$\text{Zn}(\text{CH}_3\text{COOH})_2 \cdot 2\text{H}_2\text{O}$, 0.5 M] in solvent mixture of glycerol and ethylene glycol ($\text{C}_2\text{H}_6\text{O}_2$ and $\text{C}_2\text{H}_8\text{O}_3$, 0–60% v/v) was spin-coated (4000 rpm, 2 min) onto oxidized silicon and glass substrates. The surface of the substrates was prepared previously by piranha soak, followed by 2 h soak in ethanol deionized water (1:1 v/v) solution to achieve good adhesion with the sol. The sol coated onto the substrates was hydrolyzed in humid air at 100°C, followed by bake at 150°C for 30 min to evaporate excess solvents. Pyrolysis/annealing of the hydrolyzed sol films was carried out in oxygen ambient for 30 min at 550°C. The

electrical contacts to the ZnO film were formed by the evaporation of aluminum, followed by anneal of 30 s in argon ambient at 450°C.⁷

The ZnO films were characterized by various techniques. The crystal structure and grain size of the ZnO thin films were studied by X-ray diffraction (XRD) (Philips X'Pert Pro, PANalytical B.V., The Netherlands, using Cu K α) and morphology by scanning electron microscopy (SEM) (e_LiNE, Raith, Dortmund, Germany). The film thickness was measured by ellipsometer (Sentech's SENresearch, Berlin, Germany). Photoluminescence measurements (Princeton Applied Research) were carried out using an excitation of 300 nm wavelength from a xenon short-arc lamp source at room temperature to estimate the defect levels in the ZnO film. Visible light absorption spectrum of the ZnO film was measured using Bruker (Ettlingen, Germany) IFS 66v/s (in the visible and near-infrared range of 400–1136 nm). The electrical characterization of ZnO films was performed using Agilent (Santa Clara, CA) 4155C semiconductor parameter analyzer.

Results and Discussion

The SEM micrographs of the films obtained from sols of different glycerol contents are shown in Fig. 1. The films were prepared by multiple repeated coating of the sol resulting in films thicker than 80 nm. The high magnification SEM micrographs show that the films have a porous and nonuniform morphology. The films are polycrystalline with the average grain size varying from about 45 to 78 nm. The mean grain size can be observed to increase with increasing glycerol content in the sol. The XRD plots of the films prepared by sols with different glycerol contents are shown in the inset of Fig. 2. The peaks at 2θ of 33.2 and 63.1° correspond to (002) and (103) planes of ZnO wurtzite. The peaks may be observed to become sharper with larger glycerol content in the sol. The mean grain size of the film, as inferred from the XRD plots using Debye–Scherrer relation,¹⁴ is plotted in Fig. 2 as a function of glycerol percentage in the sol. The mean grain size increases with increasing glycerol content in the sol. The influence of precursor concentration on the mean grain size is almost negligible for high glycerol sols. But the mean grain size drops for sols containing less glycerol. This result is central because it provides useful insight into the reaction kinetics.

In general, whenever the thickness of the polycrystalline film is larger than the mean grain size of the film, the average grain size can increase significantly with a slower deposition rate.¹⁵ In the present case, the rate of deposition is determined by two competing processes: the hydrolysis of the sol at the surface of the sol film that interfaces with the water-vapor saturated ambient and the diffusion of the precursor species in the sol film to these reaction sites. With more glycerol in the sol, the rates of both of these processes fall. This is because the addition of glycerol (high boiling and highly viscous) to ethylene glycol increases the boiling point and viscosity

^z E-mail: gnaik@purdue.edu

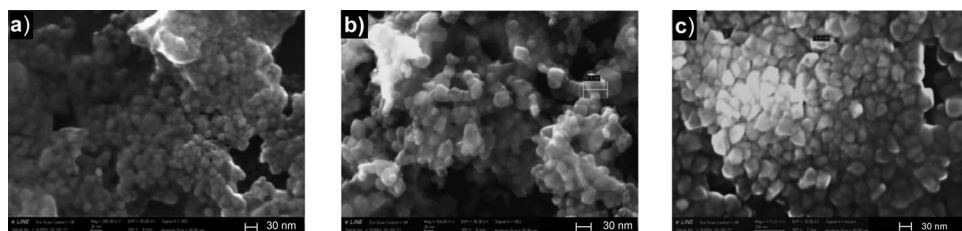


Figure 1. High resolution scanning electron micrographs of zinc oxide films deposited by sols composed of (a) no glycerol, (b) 20% glycerol, and (c) 40% glycerol.

of the sol. While the former increases the activation energy of the hydrolysis reaction, the latter decreases the mobility of the reactant species. Hence, the overall rate of deposition decreases and the mean grain size increases with more glycerol in the sol.

Thin films of ZnO prepared by a single coating of the sol were subjected to ellipsometry measurements in order to infer their thicknesses.¹⁶ The thickness of a single-spin-coated ZnO film as a function of percentage of glycerol in the sol is plotted in Fig. 3. The thickness of the ZnO film increases with increasing glycerol content. This is because the viscosity of the sol increases with higher glycerol content in the sol. On the right axis of the figure, the viscosity of the sol, as extracted using Navier–Stokes and momentum balance simplifications,¹⁷ is plotted. Greater the viscosity of the sol, thicker

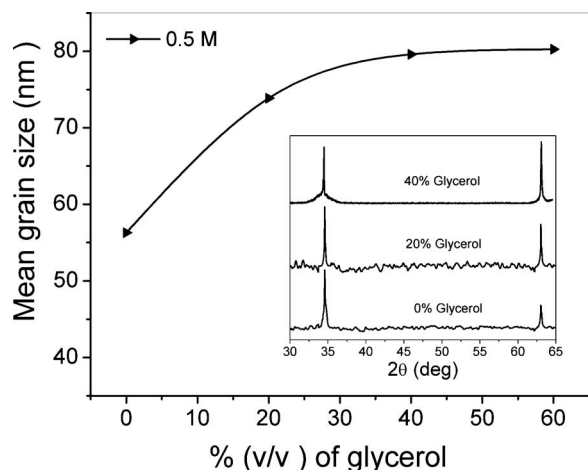


Figure 2. Mean grain size of ZnO films as extracted from XRD measurements plotted against glycerol content of the sol. The inset shows the XRD plots for zinc oxide thin films prepared by sols with different glycerol contents.

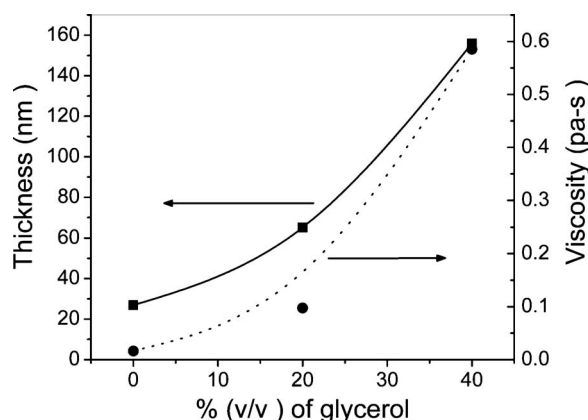


Figure 3. Thickness of zinc oxide film deposited by single spin-coating vs glycerol content in the sol. The dotted curve plots the viscosity of the sol as extracted from the Stokes–Navier approximation.

is the film of the sol spin-coated on the substrate. This translates to more precursor material deposited, which, in turn, results in a thicker ZnO film.

PL measurements at room temperature were carried out to investigate the defect structure in the ZnO films. The PL spectra of the ZnO thin films obtained from the sols of different glycerol contents are shown in Fig. 4. The room temperature bandgap of ZnO is about 3.37 eV. But the broad peak around 3.1 eV, corresponding to the blue emission, confirms that the emission is due to electronic transitions involving the defect states in the bandgap. The green emission around 2.3 eV, attributed to the common defect in the ZnO film, oxygen deficiency,^{18,19} is suppressed in these ZnO films indicating better quality of the films. The blue peak shifts from 3.105 eV for no glycerol in the sol to 3.18 eV for 40% glycerol in the sol, indicating that the defect states move closer to bandedges with higher glycerol content in the sol. Also, the intensity of PL emission decreases with more glycerol in the sol. Thus, higher glycerol sol improves the film quality. The small peak in the PL spectrum of the ZnO film obtained from 40% glycerol sol at 3.48 eV may be due to the defects formed due to strain induced cracks in the thicker film.

The optical characterization of the ZnO film deposited from the sol containing 20% glycerol is shown in Fig. 5. The ZnO film (about 60 nm thick) is more than 80% transparent in the visible spectrum. The inset of Fig. 5 plotting the square on the absorption coefficient (α) versus photon energy shows that the bandgap of the ZnO film is about 3.39 eV. The transmittance plot also provides information about the porosity of the films.²⁰ The refractive index of the film extracted from the optical characterization data is compared with that of a bulk film to obtain porosity. The porosity calculated by Lorentz–Lorentz equation²⁰ yielded an average value of about 14% for the 60 nm thick films grown from the sol containing 20% glycerol.

The electrical characteristics of the zinc oxide film prepared with

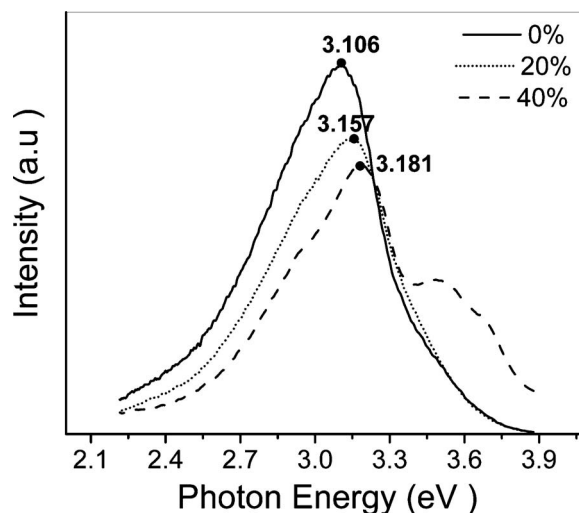


Figure 4. Photoluminescence spectra of the zinc oxide films deposited by sols composed of different glycerol concentrations.

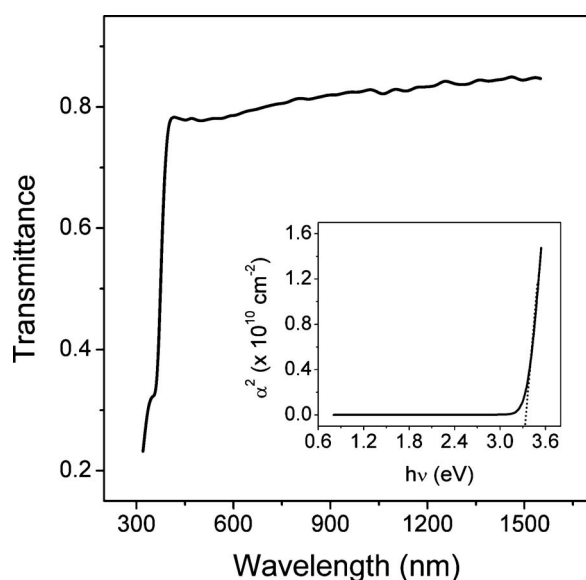


Figure 5. Transmittance spectrum of a 60 nm thick zinc oxide film spin-coated on thick glass substrate. The inset shows the square on the absorption coefficient vs photon energy.

20% glycerol were studied by forming aluminum ohmic contact pads to the 60 nm thick ZnO film. The ZnO film was deposited on a 136 nm thick silicon oxide layer thermally grown on silicon substrate. The silicon substrate was contacted to form a back-gate field-effect controlled device. The inset of Fig. 6 shows the schematic structure of this field-effect device. The current–voltage characteristics of this device for different back-gate voltages are plotted in Fig. 6. The intrinsic ZnO film with grounded back-gate exhibits specific resistivity of $291 \text{ M}\Omega/\square$ and resistivity of $18.04 \text{ }\Omega \text{ cm}$. The conductivity of the ZnO film may be observed to fall with a more negative bias on the back-gate indicating an n-type semiconducting film. The field-effect mobility,²¹ as extracted from the electrical characteristics, is $0.78 \text{ cm}^2/(\text{V s})$ at zero back-gate bias.

Conclusions

This study demonstrated that composition of the sol can have profound influence on the properties of the sol–gel deposited zinc oxide thin films. The sol–gel process based on the mixture of ethylene glycol and glycerol showed that altering the key properties of the sol such as viscosity and boiling point by simply varying the composition of the sol can significantly change the properties of the zinc oxide film, such as morphology, mean grain size, defect structure, and the thickness of the film. Thus, we demonstrated a simple technique to tune the sol–gel process for depositing zinc oxide films. This demonstration has two main consequences. First, tuning the properties of the sol–gel deposited films by altering the properties of the sol may be generalized to many materials other than zinc oxide. Second, it enables a right choice of constituents and composition of the sol by providing better understanding of the influence of param-

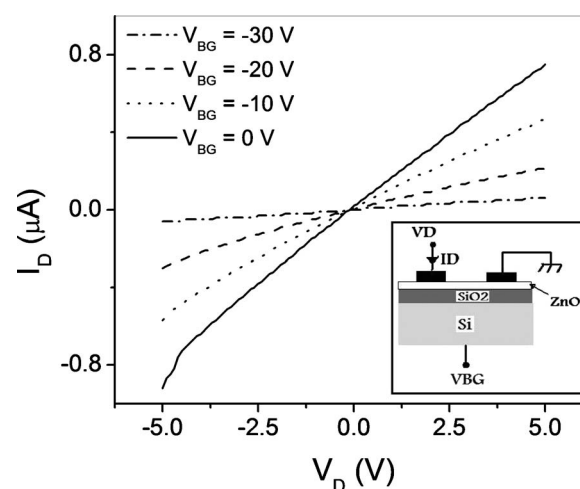


Figure 6. Current–voltage characteristics of an intrinsic zinc oxide film plotted for different back-gate biases. The inset shows the device structure and the setup for electrical characterization.

eters of the sol on reaction kinetics. The optimization of the sol composition resulted in 20% glycerol, and the optimum zinc oxide film prepared with this sol is observed to be about 80% transparent in the visible spectrum and exhibited electrical resistivity of about $18 \text{ }\Omega \text{ cm}$ and field-effect mobility of $0.78 \text{ cm}^2/(\text{V s})$.

Acknowledgment

We acknowledge the support received from Ministry of Communication and Information Technology, Government of India under the project “Center for Excellence in Nanoelectronics.”

References

- R. L. Hoffman, B. J. Norris, and J. F. Wager, *Appl. Phys. Lett.*, **82**, 733 (2003).
- R. Cebulla, R. Wendt, and K. Ellmer, *J. Appl. Phys.*, **83**, 1087 (1998).
- D. H. Kim, N. G. Cho, H. G. Kim, and W. Y. Choib, *J. Electrochem. Soc.*, **154**, H939 (2007).
- T. Saeed and P. O'Brien, *Thin Solid Films*, **271**, 35 (1995).
- M. Krunk and E. Mellikov, *Thin Solid Films*, **270**, 33 (1995).
- M. Ohyama, H. Kouzuka, and T. Yoko, *Thin Solid Films*, **306**, 78 (1997).
- D. Redinger and V. Subramanian, *IEEE Trans. Electron Devices*, **54**, 1301 (2007).
- M. N. Kamalasanan and S. Chandra, *Thin Solid Films*, **288**, 112 (1996).
- S.-Y. Chu, T.-M. Yan, and S.-L. Chen, *J. Mater. Sci. Lett.*, **19**, 349 (2000).
- B. J. Norris, J. Anderson, J. F. Wager, and D. A. Keszler, *J. Phys. D: Appl. Phys.*, **36**, L105 (2003).
- C. Y. Tsay, H. Cheng, M. Wang, P. Lee, C. Chen, and C. Lin, *Surf. Coat. Technol.*, **202**, 1323 (2007).
- S. O'Brien, L. H. K. Koh, and G. M. Crean, *Thin Solid Films*, **516**, 1391 (2008).
- M. Dutta, S. Mridha, and D. Basak, *Appl. Surf. Sci.*, **254**, 2743 (2008).
- A. L. Patterson, *Phys. Rev.*, **56**, 978 (1938).
- C. V. Thompson, *Annu. Rev. Mater. Sci.*, **20**, 245 (1990).
- P. L. Washington, H. C. Ong, J. Y. Dai, and R. P. H. Chang, *Appl. Phys. Lett.*, **72**, 3261 (1998).
- B. D. Washo, *IBM J. Res. Dev.*, **21**, 190 (1977).
- X. L. Wu, G. G. Siu, C. L. Fu, and H. C. Ong, *Appl. Phys. Lett.*, **78**, 2285 (2001).
- H. S. Kang, J. S. Kang, J. W. Kim, and S. Y. Lee, *J. Appl. Phys.*, **95**, 1246 (2004).
- S. Mridha and D. Basak, *Chem. Phys. Lett.*, **427**, 62 (2006).
- D. K. Schroder, *Semiconductor Material and Device Characterization*, p. 548, John Wiley & Sons, New York (1998).